Thermodynamic properties of the Heisenberg model on a triangular lattice with two exchange couplings: Application to two-dimensional solid ^{3}He adsorbed on graphite

Takashi Koretsune,[1] Masafumi Udagawa,[2] and Masao Ogata[3]
[1]*Department of Physics, Tokyo Institute of Technology, Meguro-ku, Tokyo 152-8551, Japan*
[2]*Department of Applied Physics, University of Tokyo, Bunkyo-ku, Tokyo 113-8656, Japan*
[3]*Department of Physics, University of Tokyo, Bunkyo-ku, Tokyo 113-0033, Japan*
(Received 10 January 2009; revised manuscript received 6 July 2009; published 7 August 2009)

To discuss the gapless spin-liquid-like behavior of the second-layer solid-phase ^{3}He adsorbed on graphite, we study a spin-1/2 Heisenberg model on a triangular lattice with two kinds of superexchange couplings due to the corrugation effects from the first-layer by using finite temperature Lanczos method and high-temperature expansions. In some parameter region, it is found that this model can be expressed by an effective Hamiltonian with two different energy scales consisting of kagomé Heisenberg model and triangular Heisenberg model. We find that this effective Hamiltonian well reproduces the experimental behaviors such as the double-peak structure and the low-temperature linear-T behavior of the specific heat as well as the excess enhancement of the spin susceptibility at low temperatures.

DOI: 10.1103/PhysRevB.80.075408 PACS number(s): 67.30.ej, 75.10.Jm, 75.70.Ak

Resonating valence bond (RVB) state, considered to be a typical spin liquid state, was first proposed by Anderson for the Heisenberg model on a triangular lattice.[1] Since then, the effect of geometrical frustration and possibility of spin liquid states in strongly correlated systems have been long standing problems in condensed-matter physics.[2] In general, frustration suppresses conventional long-range orders such as antiferromagnetism and charge order and lowers the transition temperatures in many cases. Recently several materials have been found to exhibit spin-liquid-like behavior without any trivial phase transition.

^{3}He atoms adsorbed on a graphite are considered to form an ideal two-dimensional system with nuclear spin $S=1/2$.[3] In the registered phase of the second layer of ^{3}He, or the so-called 4/7 phase, ^{3}He atoms on a first layer of ^{3}He or ^{4}He or on a bilayer of HD form a triangular lattice. The simplest model for this system is, thus, the Heisenberg model on a triangular lattice. Specific heat measurement of this system shows a double peak structure and behaves as $C_V \propto T$ below the lower peak.[3] However, these behaviors contradict the theoretical results for the simple triangular Heisenberg model, i.e., the stabilization of 120° antiferromagnetic long range order[4] and the spin-wave-like temperature dependence of specific heat: $C_V \propto T^2$ at low temperature below a single peak.[5–7] The experimentally observed behavior of $C_V \propto T$ indicates the absence of long-range order. Furthermore, NMR experiment[8] shows that the magnetization, which corresponds to the uniform spin susceptibility, has an enhancement from Curie-Weiss laws at low temperatures and increases gradually down to about 10 μK without any signals of phase transition nor spin gap. These spin-liquid-like behaviors have not been understood theoretically. In this paper, we propose a mechanism which explains both behaviors of specific heat and uniform spin susceptibility.

So far, two spin models have been employed to study this system. One is to start from a kagomé lattice.[9] In this approach, the triangular lattice of ^{3}He is divided into two parts (Fig. 1), namely, a kagomé lattice (called A site in the following) and the remaining non-kagomé lattice (called B site). B sites form a triangular lattice by themselves. The interaction with the first layer gives different potential energies to the A and B sublattices. The difference of potential energies leads to the inequivalence of Heisenberg superexchange couplings J' (between A and B site) and J (between the A sites). If we assume that the Heisenberg superexchange coupling, J', can be neglected compared with the coupling, J, the system is approximated as a Heisenberg model on the kagomé lattice with only the A sites. In fact, this approach was adopted in Ref. 10 to explain the origin of missing entropy; that is, the early specific heat measurement had shown that the entropy of the second layer ^{3}He falls short of the expected value of $k_B \ln 2$. However, precise measurement down to low temperatures revealed that there are no missing entropy.[3] This means that the effect of J' should be taken into account to explain the overall specific-heat measurement. Although the effect of J' has been studied by several groups,[11–14] they are not sufficient to explain the experimental results.

The second approach is to use multiple exchange interactions.[15–20] In this model, the competition between the nearest-neighbor ferromagnetic exchange coupling and the four-spin ring exchange interactions tends to prevent a formation of magnetic order. Although double peak structure of specific heat can be understood in this model and interesting phases are predicted theoretically,[16,19] the exact diagonalization study[18] shows that the state without magnetic order has a finite spin gap, which contradicts with the gapless-like behavior observed in the NMR experiment. The effect of multiple exchange interactions has also been studied outside the 4/7 phase.[20] Once mobile vacancies are introduced to the 4/7 phase, the difference between the A and B sites becomes smeared out and the ring exchange interactions will become important. In this paper, we focus on the 4/7 phase without mobile vacancies emphasizing the effect of the difference of A and B sites, compared with the ring exchange interactions, to study the spin-liquid-like behavior. In the parameter region where coupling between the A and B sites can be treated as a perturbation, we derive an effective Hamiltonian and

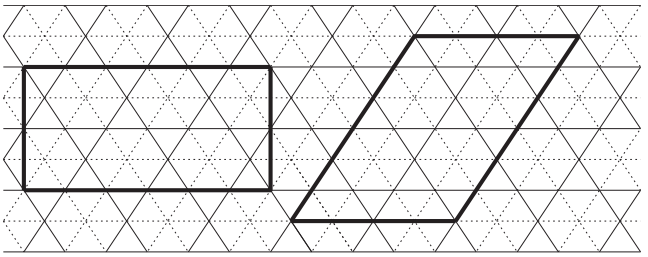

FIG. 1. Triangular lattice with two exchange couplings used in this study. Thin solid lines represent the bonds between A sites forming a kagomé lattice, and thin dashed lines represent the bonds between A sites and the remaining sites (B sites). B sites form a triangular lattice by themselves. The bold solid lines indicate two 24-site clusters used in the exact diagonalization study.

find that this effective Hamiltonian clearly explains the specific heat and NMR experiments of the second layer ^{3}He at low temperatures.

With the four-spin ring exchange interactions, the Hamiltonian is given as

$$H = J\sum_{\langle ij\rangle} \boldsymbol{S}_i \cdot \boldsymbol{S}_j + J'\sum_{\langle ij\rangle} \boldsymbol{S}_i \cdot \boldsymbol{S}_j + K\sum_{\square} (P_{ijkl} + P_{ijkl}^{-1}), \quad (1)$$

where the first summation $\langle ij\rangle$ is taken over the bonds between the A sites (the kagomé lattice) and the second summation $\langle ij\rangle'$ over the bonds between the A and B sites (Fig. 1). The last summation is taken over all the plaquettes consisting of the nearest-neighbor bonds and P_{ijkl} represents the four-spin ring exchange operator. Note that three-spin ring exchanges, which can be expressed as ferromagnetic two-spin Heisenberg interaction, are included in J and J'. Note also that, the three and four-spin ring exchange interactions are equivalent in all the plaquettes even with the corrugation effect. Thus, the model parameter J'/J in this effective Hamiltonian can take small or even negative values depending on the ratio of the Heisenberg and three-spin ring exchange interactions. Hereafter, we will set the Boltzmann factor k_B equal to unity.

Firstly, we consider the case with $K=0$. The effect of K will be briefly discussed later. In the case of $K=0$ and $J'/J=0$, the model is decoupled into the Heisenberg model on the kagomé lattice (A sites) and free spins on the remaining sites (B sites), and the model becomes a uniform Heisenberg model on the triangular lattice at $J'/J=1$. First we calculate the specific heat and spin susceptibility by using the finite temperature Lanczos method (FTLM)[21] in the two types of 24-site clusters shown in Fig. 1. To reduce boundary effects at low temperatures, we take average over boundary conditions.[22] Fig. 2(a) shows the obtained results of the specific heat, C_V, for several values of J'/J. For the case of kagomé lattice ($J'/J=0$), C_V shows a double-peak structure. The sharp peak at low temperature ($T/J\sim 0.1$) indicates the existence of highly degenerate low-lying states. However, the exact diagonalization study[23] has shown that the kagomé Heisenberg model has a finite spin gap, so that this does not explain the gapless-like behavior of spin excitations observed in the magnetization experiment of ^{3}He.

As J'/J increases, the double-peak structure gradually changes into a single-peak with a shoulder. Here, we note that the behavior of C_V for $J'/J\leq 0.2$ is qualitatively different from that of $J'/J>0.2$. C_V is almost independent of J' at high temperatures for $J'/J\leq 0.2$. This indicates that the entropy due to the B-site spins is released only at low temperatures and that the thermodynamic behavior is mostly determined by the kagomé Heisenberg model in a broad temperature range. The degeneracy of B-site spins is lifted with a small energy scale. For $J'/J>0.2$, on the other hand, C_V depends on J' in a whole temperature range.

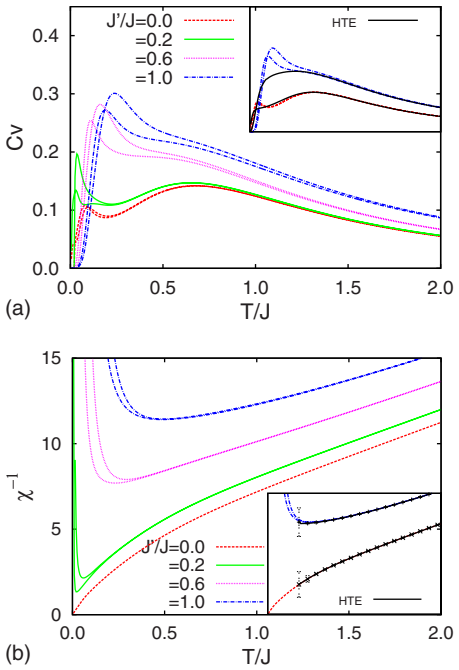

FIG. 2. (Color online) (a) Specific heat, C_V, and (b) inverse of spin susceptibility, χ^{-1}, at $J'/J=0.0$, 0.2, 0.6, and 1.0 (from bottom to top) on the two types of 24-site clusters obtained in the FTLM. Insets of (a) and (b) show the comparison of HTE (black solid line) and FTLM results at $J'/J=0.0$ and 1.0 in the same temperature range, i.e., $0\leq T/J\leq 2.0$. Error bars of the HTE results are determined from the scattering of various Padé approximations.

Let us compare the results of the FTLM with those obtained in the high-temperature expansion (HTE).[7] The inset of Fig. 2(a) shows a comparison of HTE (black solid line)[5,7,24–26] and FTLM at $J'/J=0$ and 1. To extrapolate the high-temperature series of specific heat down to low temperatures, we use the Padé approximation of $S(E)^p$.[7,27] Here, p determines the low temperature behavior as $S(T)=T^{1/(p-1)}$. In the triangular lattice, we assume the 120° Néel order and take $p=3/2$.[7] In the kagomé lattice, however, due to the many low-lying singlet excitations, the thermodynamic properties at low temperatures have not been clarified yet. Here, we assume $S(T)\propto T$ and take $p=2$. The assumption of this low-temperature property does not change the following discussions. The differences caused by other choices of p have been discussed in Ref. 24. As shown in the inset of Fig. 2(a), HTE results coincide with FTLM results except for the low-temperature peak in the case of the triangular lattice ($J'/J=1$). In particular, at low temperatures in the kagomé lattice, both methods consistently show the double peak structure.

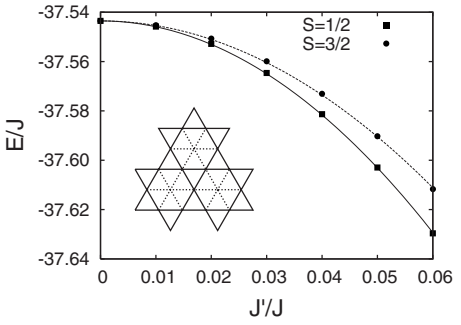

FIG. 3. Energies of the ground state and first excited state in the 27-site cluster shown in the inset. Data are fitted by quadratic functions.

This guarantees the reliability of the present FTLM especially for small values of J'. On the other hand, the difference between the FTLM and HTE method in the triangular lattice probably indicates that 24-site cluster is not appropriate to treat the antiferromagnetic 120° structure. In fact, low-energy excitation in the FTLM result shows gapful behavior rather than the expected spin-wave behavior.

Next let us discuss spin susceptibility, χ, defined by $\chi = \Sigma_{ij}\langle S_i^z \cdot S_j^z\rangle / T$. Figure 2(b) shows χ^{-1} for several values of J'/J obtained by the FTLM. In this case, the FTLM results coincide very well with HTE results as shown in the inset of Fig. 2(b), although the HTE method cannot be extended to lower temperatures as $T/J < 0.3$. For the case of kagomé lattice ($J'/J=0$), χ diverges as the temperature approaches zero ($T \to 0$), due to the free spins in the B sites. Furthermore, we find that χ shows an enhancement from the Curie-Weiss law at low temperatures, i.e., χ^{-1} becomes smaller than the high-temperature Curie-Weiss behavior, $\chi^{-1} = (T+\Theta_W)/C$, where Θ_W and C represent the Weiss temperature and Curie constant, respectively. This behavior can also be attributed to the free spins on the B sites. The behavior of χ^{-1} for $J'/J \leq 0.2$ can be understood as a continuation of $J'/J=0$ except for the very low temperatures. In this region, χ still shows an enhancement from the Curie-Weiss law, as shown in Fig. 2(b). This nearly-free-spin behavior of B sites is consistent with the specific heat behavior in Fig. 2(a), where the degeneracy of the B-site spins is lifted with a small energy scale. Therefore, both specific heat and magnetic susceptibility give a consistent result with the experiments for $J'/J \leq 0.2$.

Motivated by the consistency with the experiments, we focus on the case of $J'/J < 0.2$ in the following. At $J'/J=0$, spins on the kagomé lattice (A site) and B site are decoupled. Thus, the effect of J' can be treated as a perturbation. Since the kagomé Heisenberg model probably has a small but finite spin gap,[23] we assume that the perturbation only lifts the degeneracy of the free spins on the B sites and has little effect on the kagomé Heisenberg spins. This perturbative effect of the lowest order can be expressed by an effective exchange coupling, $J_{\rm eff}$, between the free spins. To extract $J_{\rm eff}$, we study a cluster with 27-sites with open boundary conditions as shown in Fig. 3 and diagonalize the Hamiltonian using exact diagonalization method. In the small-J' region, the low-energy spectrum of this system can be approximated by the three-site Heisenberg model with the exchange coupling, $J_{\rm eff}$. Then the energy of ground state and first excited states of these three spins become $E_0 = -\frac{3}{4}J_{\rm eff}$ and $E_1 = \frac{3}{4}J_{\rm eff}$, respectively. Therefore, one can extract the value of $J_{\rm eff}$ from $E_1 - E_0$ obtained by exact diagonalization. The energies of the ground state and the first excited state are shown in Fig. 3 as a function of J'/J. The obtained ground state and the first excited states are both spin quartets with $S=1/2$ and $S=3/2$, respectively, justifying the approximation by three-site Heisenberg model. Therefore, the energy difference in Fig. 3 corresponds to $E_1 - E_0 = \frac{3}{2}J_{\rm eff}$. By fitting the energy difference in a quadratic function of J'/J, we obtain $E_1 - E_0 = 5.04J'^2/J$. From this, we estimate the effective coupling, $J_{\rm eff}$, as $J_{\rm eff} = 3.4J'^2/J$.

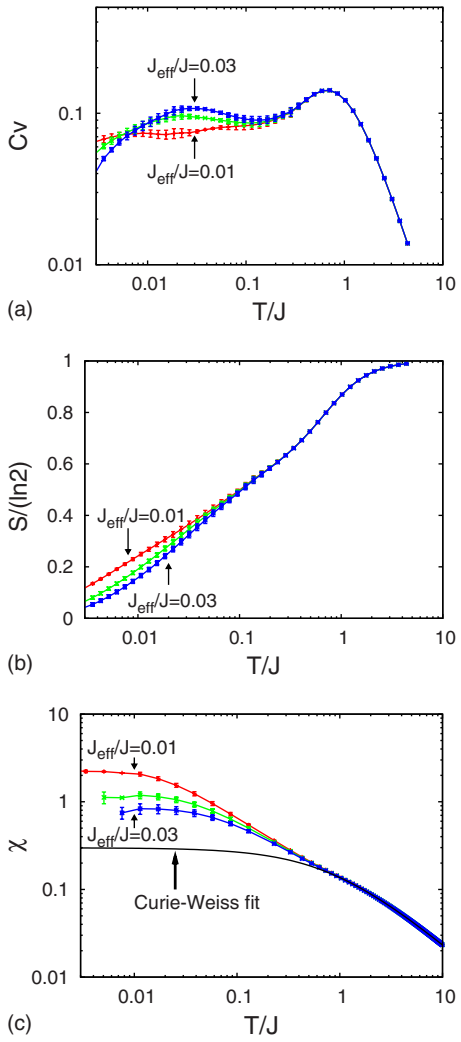

FIG. 4. (Color online) (a) Specific heat, (b) entropy, and (c) spin susceptibility for the effective Hamiltonian, Eq. (2), at $J_{\rm eff}/J=0.01$, 0.02 and 0.03. For the spin susceptibility, Curie-Weiss law fitted at high temperatures is also shown by a black solid line.

As discussed above, we consider that, at least in the small J'/J region, the Hamiltonian (1) can be decoupled into kagomé Heisenberg model with the interaction, J, and triangular Heisenberg model with the effective interaction, $J_{\rm eff}$. We assume that the 4/7 phase of ^{3}He belongs in this region and use this effective Hamiltonian to describe the low-

temperature behaviors. Then, the free energy of this effective Hamiltonian becomes

$$F_{\mathrm{tot}} = \frac{1}{4}F_{\mathrm{tri}}(J_{\mathrm{eff}}) + \frac{3}{4}F_{\mathrm{kag}}(J), \tag{2}$$

where $F_{\mathrm{tri}}(J)$, $F_{\mathrm{kag}}(J)$, and F_{tot} are the free energies of the triangular Heisenberg model, kagomé Heisenberg model, and the total model Hamiltonian, respectively. For $F_{\mathrm{tri}}(J)$ and $F_{\mathrm{kag}}(J)$, we use the HTE results which are shown in Fig. 2. Figure 4 shows the specific heat, entropy and spin susceptibility obtained in this effective Hamiltonian at $J_{\mathrm{eff}}/J = 0.01-0.03$. One can see that the specific heat shows a double-peak structure for $J_{\mathrm{eff}}/J = 0.02-0.03$. In general, there should be three peaks in the specific heat; two peaks from the kagomé Heisenberg model and one peak from the triangular Heisenberg model with J_{eff}. However, in this parameter range, the lower peak of the kagomé Heisenberg model and that of the triangular Heisenberg model are in the same temperature region. Therefore, these two peaks cannot be distinguished any more. Note that the differences of C_V (and S) between different values of J_{eff}/J purely come from the contributions of the triangular lattice. (There is no contribution to C_V at finite temperatures when $J_{\mathrm{eff}}=0$.) We expect that the second layer ^{3}He corresponds to the case with $J_{\mathrm{eff}}/J = 0.02-0.03$ where the specific heat has only two peaks. From the temperature dependence of entropy shown in Fig. 4(b), we can see that the entropy from the triangular Heisenberg model is released around the lower peak of C_V. Note that it is rather difficult to conclude the behavior of $C_V \propto T$ below the lower peak, since the low-energy structure of C_V is a combination of kagomé and triangular Heisenberg models within the current temperature range. Nevertheless, we speculate that a combination of the highly degenerate behavior of C_V from the kagomé lattice and the behavior of $C_V \propto T^2$ from the low-temperature triangular lattice can lead to the linear-T behavior of C_V.

The spin susceptibility, χ, shown in Fig. 4(c) also seems consistent with the experiments. At low temperatures, χ exceeds the Curie-Weiss law fitted at high temperatures (black solid line). This is because the spin susceptibility of the triangular lattice, which has a small Weiss temperature, becomes dominant at low temperatures. Note that this characteristic feature of the spin susceptibility is described by the superposition of two Curie-Weiss curves with different Curie constants and Weiss temperatures. The saturation of χ at low temperatures is determined by the triangular Heisenberg model, since the kagomé Heisenberg model has a finite spin gap as discussed before. Actually, the saturation occurs around $T/J_{\mathrm{eff}} = 0.2-0.3$, which is far smaller than J, consistent with experiments.[8] The saturation value depends on J_{eff}.

Finally, we discuss the effect of four-spin ring exchange interactions, K. This term can be rewritten by the spin operators as

$$P_{1234} + P_{1234}^{-1} = \sum_{1\le i<j\le 4} \boldsymbol{S}_i \cdot \boldsymbol{S}_j + 4[(\boldsymbol{S}_1 \cdot \boldsymbol{S}_2)(\boldsymbol{S}_3 \cdot \boldsymbol{S}_4) + (\boldsymbol{S}_1 \cdot \boldsymbol{S}_4) \times (\boldsymbol{S}_2 \cdot \boldsymbol{S}_3) - (\boldsymbol{S}_1 \cdot \boldsymbol{S}_3)(\boldsymbol{S}_2 \cdot \boldsymbol{S}_4)]. \tag{3}$$

If the effect of this term is small, the mean-field treatment such as

$$(\boldsymbol{S}_1 \cdot \boldsymbol{S}_2)(\boldsymbol{S}_3 \cdot \boldsymbol{S}_4) \sim \langle \boldsymbol{S}_1 \cdot \boldsymbol{S}_2 \rangle \boldsymbol{S}_3 \cdot \boldsymbol{S}_4 + \langle \boldsymbol{S}_3 \cdot \boldsymbol{S}_4 \rangle \boldsymbol{S}_1 \cdot \boldsymbol{S}_2 - \langle \boldsymbol{S}_1 \cdot \boldsymbol{S}_2 \rangle \times \langle \boldsymbol{S}_3 \cdot \boldsymbol{S}_4 \rangle \tag{4}$$

will be valid and all the terms can be represented as two-spin exchange interactions. Furthermore, since the coefficients of the exchange coupling terms on the next-nearest-neighbor sites are small compared to those on the nearest-neighbor sites,[28] the effect of the ring exchange interaction can be absorbed in the effective J_{eff} and J in the first approximation. As far as K is not so large, we speculate that the effect beyond this approximation can be treated perturbatively and that the present results do not change qualitatively. If K is larger than about $J/10$, it has been discussed that a different state such as resonating valence bond state can be realized.[18,20] The effect of the long-range exchange interactions can also be important as discussed in the classical limit[29] and should be clarified in future studies.

The characteristic property of this effective model is the magnetic response. If the present assumption is valid, the spins on the triangular lattice (B sites) highly respond to the applied magnetic field since the effective coupling, J_{eff}, is small compared to J. This means that in the intermediate magnetic field there is a characteristic region where 1/4 of total spins are polarized. In addition to this possible structure at 1/4, magnetization curve of the effective model will have a plateau at 1/2 ($=1/4+3/4\times 1/3$) of the full magnetization since kagomé lattice Heisenberg model itself has a magnetization plateau at 1/3 of its full magnetization.[30] These two characteristic regions in the magnetization curve is consistent with the recent experiment.[31]

Although the low-temperature behaviors of C_V and χ in the present model agree well with the experiments, there is a discrepancy between theory and experiment. In the experiment,[3] the specific heat at high-temperature region decays slowly and does not behave as $C_V \propto T^{-2}$, while within the usual spin Hamiltonians, C_V always behaves as $C_V \propto T^{-2}$. In fact, the high-temperature behavior of C_V in Fig. 4(a) is $C_V \propto T^{-2}$. In order to understand the experimentally observed behavior of C_V, it will be necessary to take into account the effect of mass degrees of freedom[32] such as the interstitial sites in the second layer of ^{3}He and/or the excitation to the third layer.

To summarize, we analyzed the 4/7 phase of ^{3}He adsorbed on graphite using the Heisenberg model on the lattice that interpolates between the triangular and the kagomé lattices. We found that at $J'/J < 0.2$, this model can be decoupled into two Hamiltonians with different energy scales and that this decoupling explains the experimental properties such as the double peak and the low-temperature linear-T behavior of the specific heat as well as the excess enhancement of the spin susceptibility at low temperatures.

The authors would like to thank H. Fukuyama, Y. Matsumoto, and T. Momoi for useful discussions. This work was partially supported by Grant-in-Aid for Scientific Research from MEXT Japan (Grant No. 17071002) and also by a Next Generation Supercomputing Project, Nanoscience Program, MEXT, Japan.

[1] P. W. Anderson, Mater. Res. Bull. **8**, 153 (1973).
[2] *Frustrated Spin Systems*, edited by H. Diep (World Scientific, Singapore, 2005).
[3] K. Ishida, M. Morishita, K. Yawata, and H. Fukuyama, Phys. Rev. Lett. **79**, 3451 (1997).
[4] B. Bernu, P. Lecheminant, C. Lhuillier, and L. Pierre, Phys. Rev. B **50**, 10048 (1994).
[5] N. Elstner, R. R. P. Singh, and A. P. Young, Phys. Rev. Lett. **71**, 1629 (1993).
[6] A. E. Trumper, L. Capriotti, and S. Sorella, Phys. Rev. B **61**, 11529 (2000).
[7] T. Koretsune and M. Ogata, Phys. Rev. Lett. **89**, 116401 (2002); J. Phys. Soc. Jpn. **72**, 2437 (2003).
[8] R. Masutomi, Y. Karaki, and H. Ishimoto, Phys. Rev. Lett. **92**, 025301 (2004).
[9] V. Elser, Phys. Rev. Lett. **62**, 2405 (1989).
[10] D. S. Greywall and P. A. Busch, Phys. Rev. Lett. **62**, 1868 (1989).
[11] C. Zeng and V. Elser, Phys. Rev. B **42**, 8436 (1990).
[12] Y. R. Wang, Phys. Rev. B **45**, 12608 (1992).
[13] D. J. J. Farnell, R. F. Bishop, and K. A. Gernoth, Phys. Rev. B **63**, 220402(R) (2001).
[14] L. Arrachea, L. Capriotti, and S. Sorella, Phys. Rev. B **69**, 224414 (2004).
[15] M. Roger, Phys. Rev. Lett. **64**, 297 (1990).
[16] T. Momoi, K. Kubo, and K. Niki, Phys. Rev. Lett. **79**, 2081 (1997).
[17] M. Roger, C. Bäerle, Y. M. Bunkov, A.-S. Chen, and H. Godfrin, Phys. Rev. Lett. **80**, 1308 (1998).
[18] G. Misguich, C. Lhuillier, B. Bernu, and C. Waldtmann, Phys. Rev. B **60**, 1064 (1999).
[19] T. Momoi, P. Sindzingre, and N. Shannon, Phys. Rev. Lett. **97**, 257204 (2006).
[20] Y. Fuseya and M. Ogata, J. Phys. Soc. Jpn. **78**, 013601 (2009).
[21] J. Jaklič and P. Prelovšek, Adv. Phys. **49**, 1 (2000).
[22] Average is taken over 64 boundary conditions for 24-site clusters, which is confirmed to be sufficient.
[23] C. Waldtmann, H.-U. Everts, B. Bernu, C. Lhuillier, P. Sindzingre, P. Lecheminant, and L. Pierre, Eur. Phys. J. B **2**, 501 (1998).
[24] G. Misguich and B. Bernu, Phys. Rev. B **71**, 014417 (2005).
[25] C. Domb and M. S. Green, *Phase Transitions and Critical Phenomena* (Academic, London, 1974), Vol. 3.
[26] N. Elstner and A. P. Young, Phys. Rev. B **50**, 6871 (1994).
[27] B. Bernu and G. Misguich, Phys. Rev. B **63**, 134409 (2001).
[28] G. Misguich, B. Bernu, and C. Lhuillier, J. Low Temp. Phys. **110**, 327 (1998).
[29] A. B. Harris, C. Kallin, and A. J. Berlinsky, Phys. Rev. B **45**, 2899 (1992).
[30] K. Hida, J. Phys. Soc. Jpn. **70**, 3673 (2001).
[31] H. Nema, A. Yamaguchi, T. Hayakawa, and H. Ishimoto, Phys. Rev. Lett. **102**, 075301 (2009).
[32] S. Watanabe and M. Imada, J. Phys. Soc. Jpn. **76**, 113603 (2007).